Polymer 68 (2015) 270–278

Contents lists available at ScienceDirect

Polymer

journal homepage: www.elsevier.com/locate/polymer

A facile approach to catechol containing UV dismantlable adhesives

Yao-Zong Wang, Lei Li, Fu-Sheng Du*, Zi-Chen Li*

Beijing National Laboratory for Molecular Sciences (BNLMS), Key Laboratory of Polymer Chemistry & Physics of Ministry of Education, College of Chemistry and Molecular Engineering, Center for Soft Matter Science and Engineering, Peking University, Beijing 100871, China

ARTICLE INFO

Article history:
Received 7 February 2015
Received in revised form
3 May 2015
Accepted 16 May 2015
Available online 21 May 2015

Keywords:
UV degradation
Catechol
Adhesive

ABSTRACT

We report a facile synthetic approach to a new type of catechol containing UV dimantlable adhesive. A series of linear polymers containing pendent catechol moieties and main chain *o*-nitrobenzyl ester groups were synthesized by the Passerini multicomponent polymerization (MCP) of a di-*o*-nitrobenzaldehyde, 1,6-diisocyanohexane, 3-(3,4-dihydroxyphenyl) propionic acid, and undecanoic acid. The content of the catechol moieties was adjusted by varying the molar ratio of 3-(3,4-dihydroxyphenyl) propionic acid to undecanoic acid. The thermal properties of these polymers were investigated, they are stable up to 250 °C, and the glass transition temperatures (T_g) are in the range of 17–70 °C. Increasing the catechol content will increase the T_g and slightly decrease the thermal stability. The pendent catechol groups and the *in situ* formed *o*-nitrobenzyl ester linkages in the polymer main chain endow the polymer with dual functions, substrate adhesiveness and UV degradation. The UV degradation process was monitored by ^{1}H NMR, GPC, UV–Vis and FTIR. Lap shear strength tests revealed that the adhesion performance of these polymers could be tuned by varying the catechol contents. UV irradiation could cleave the polymer chains, thus decreasing the adhesion strength.

1. Introduction

Adhesives are such materials that can hold different substrates together. Every year, quantities of adhesives are produced worldwide to meet different demands in industry, medicine and daily use. In fact, human beings have used natural glues such as starch or hydrolyzed collagen long before, many of which are still being used today [1]. However, with the development of adhesion technology, more and more attentions have been paid to synthetic adhesives. Because of the ease to finely tune the chemical compositions of synthetic polymers, which is a major factor influencing the adhesion strength, scientists can design better adhesives for different purposes. One such good example is the mimicry of bio-adhesives inspired by marine mussels [2–18]. These organisms are able to attach themselves firmly to the underwater surface by secreting adhesive proteins containing unique amino acid 3,4-dihydroxyphenylalanine (DOPA) [19,20]. Studies have revealed that DOPA moieties have extensive interactions with virtually any substrates via metal chelation, oxidation and Michael adduct formation etc [21–23]. Though the incorporation of DOPA or its derivatives into polymers as new functional materials has been pursued for many years, the synthetic pathway is rather complicated, often requiring complex synthetic routes and protection–deprotection procedures [2–5].

On the other hand, facile debonding ability after use is another aspect of adhesive research. This emerging area promises smart adhesives with great industrial potentials not only in terms of saving energy but also recycling materials. As can be expected, dismantlable adhesives require external stimuli, such as heat [24–34], light [35–37] and electrostatic interactions [38] to achieve the on-demand disassembly. Among them, photo irradiation is particularly attractive, because of its temporal and spatial control [39–43], which ensures precise and selective removal of adhesives. Ideally, this method provides an opportunity for easy operation and minimal damage to the substrates. A common strategy toward light responsiveness is the incorporation of *o*-nitrobenzyl ester groups in polymers [44–46]. This photolabile structure undergoes photocleavage and generates an *o*-nitrosobenzaldehyde and a carboxylic acid upon UV irradiation [47,48], which in turn changes the material properties.

However, it remains difficult to simultaneously introduce catechol moieties and *o*-nitrobenzyl ester groups into polymer through conventional synthetic procedures. An intriguing methodology is the use of multicomponent reactions (MCRs) [49–54]. Unlike

---

* Corresponding authors.
E-mail addresses: fsdu@pku.edu.cn (F.-S. Du), zcli@pku.edu.cn (Z.-C. Li).

http://dx.doi.org/10.1016/j.polymer.2015.05.032

traditional two component reactions, the fundamental superiority of MCRs is the simultaneous incorporation of more than two starting materials into a single product, providing a chance to circumvent the aforementioned problems.

Passerini reaction is a typical isocyanide based multicomponent reaction. First reported in 1921 [52], this three component reaction can assemble a carboxylic acid, an isocyanide and an aldehyde into an α-acyloxy amide in an atom-economic way. Thanks to the mild reaction conditions and functional group tolerance, our group [55–62] and others [63–69] have exploited this reaction in many aspects such as polymerization and post-functionalization. Our recent works demonstrated that the multicomponent polymerization (MCP) of a diisocyanide, a dicarboxylic acid and an *o*-nitrobenzaldehyde was a straightforward way to synthesize photocleavable polymers [59,60]. The key point was the in-situ formed o-nitrobenzyl ester linkage in the polymer main chain, this linkage can be cleaved upon UV irradiation. We here report that two functionalities, catechol and *o*-nitrobenzyl ester groups, can be simultaneously incorporated into a linear polymer via the MCP of a di-*o*-nitrobenzaldehyde derivative, 1,6-diisocyanohexane, and 3-(3,4-dihydroxyphenyl) propionic acid (Scheme 1). The facilely obtained polymers show good adhesion and UV debonding abilities, and they are expected to be used as dismantlable adhesives.

2. Experimental section

2.1. Materials

The following chemicals were used as received: 5-hydroxy-2-nitrobenzaldehyde (99%, Beijing Datianfengtuo Chem. Co., Ltd.), bromoethane (A. R., Tianjin Guangfu Fine Chem. Res. Inst.), 1, 12-dibromododecane (98%, Alfa Aesar), 1,6-diisocyanohexane (98%, Alfa Aesar), *tert*-butyl isocyanide (98%, Alfa Aesar), 3-(3,4-dihydroxyphenyl) propionic acid (98+%, Alfa Aesar), undecanoic acid (98%, Alfa Aesar). All other chemicals were purchased from Beijing Chem. Reagent Co. and used as received unless otherwise noted. THF was refluxed with Na and distilled before use.

2.2. General measurements and characterization

^{1}H NMR (300 MHz) spectra were recorded in CDCl$_3$ or DMSO-d_6 on a Varian Gemini 300 spectrometer with tetramethylsilane (TMS) as the internal reference for chemical shifts (δ, ppm). Molecular weights and polydispersity index (PDI = M_w/M_n) of polymers were measured with a gel permeation chromatography (GPC) equipped with a 2414 refractive index detector, a Waters 1525 binary HPLC pump, and three Waters Styragel HT columns (HT2, HT3, HT4). The columns were thermostated at 35 °C and THF was used as an eluent at a flow rate of 1.0 mL/min. Calibration was made against linear polystyrene standards. Thermal gravimetric analysis (TGA) was carried out using a Q600-SDT thermogravimetric analyzer (TA Co., Ltd.) with nitrogen purging rate set at 50 mL/min. Measurements were conducted from room temperature to 600 °C at a heating rate of 10 °C/min. Calorimetric measurement was performed using a Q100 differential scanning calorimeter (TA Co., Ltd.) with nitrogen purging rate set at 50 mL/min. The program was set to finish two cycles in a temperature range of −80 to 200 °C at a heating/cooling rate of 10 °C/min. Data of the endothermic curve were acquired from the second scan for each polymer sample. TA Universal Analysis software was applied for data acquisition and processing in the two measurements.

2.3. Synthesis of 5-ethoxy-2-nitrobenzaldehyde

5-Hydroxy-2-nitrobenzaldehyde (1.6712 g, 10 mmol), bromoethane (1.6346 g, 15 mmol) and potassium carbonate (1.6583 g, 12 mmol) were dissolved in DMF (20 mL). The reaction mixture was heated at 30 °C for 24 h. The excess bromoethane was evaporated under reduced pressure and the residue was poured into water to precipitate the product. After filtration, simply washing with water for three times offered 5-ethoxy-2-nitrobenzaldehyde as a pale yellow solid in 77% yield. T_m = 63 °C (Fig. S1).

2.4. Synthesis of di-o-nitrobenzaldehyde derivative monomer **1**

1, 12-dibromo-dodecane (1.6407 g, 5 mmol), 5-hydroxy-2-nitrobenzaldehyde (2.5068 g, 15 mmol), and potassium carbonate

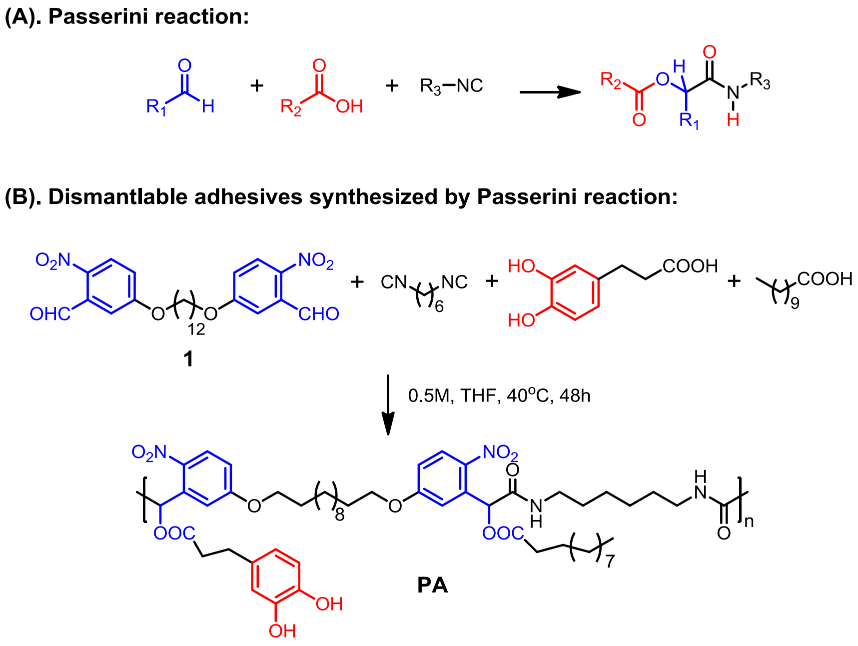

Scheme 1. Synthetic strategy for the dismantlable adhesives.

(2.0729 g, 15 mmol) were dissolved in DMF (30 mL). The reaction mixture was heated at 30 °C for 24 h, and then poured into water. The aqueous phase was extracted with CH_2Cl_2 for three times. After evaporation of CH_2Cl_2, yellow oil was obtained which was solidified after being cooled to 0 °C. Simply washing the solid with cold diethyl ether gave the di-*o*-nitrobenzaldehyde **1** as a pale yellow solid in 52% yield. $T_m = 92$ °C (Fig. S2).

2.5. Synthesis of model compound 2

3-(3,4-Dihydroxyphenyl) propionic acid (182.18 mg, 1 mmol), 5-ethoxy-2-nitro-benzaldehyde (195.17 mg, 1 mmol) and *tert*-butyl isocyanide (99.756 mg, 1.2 mmol) were dissolved in THF (1 mL). The homogeneous solution was heated to 40 °C for 48 h. During this period, the mixture gradually became heterogeneous, indicating the formation of the product. Finally, the mixture was poured into diethyl ether. The precipitated products were collected by filtration and washed with diethyl ether for three times to get compound **2** as a pale yellow solid in 80% yield. No T_m was detected for this compound.

2.6. General procedure for the Passerini MCP

In a polymerization tube containing a stir bar, carboxylic acid (total 1 mmol) with variable catechol feed ratios (3-(3,4-dihydroxyphenyl) propionic acid: undecanoic acid = 0:10, 1:9, 2:8, 3:7, 4:6, 5:5, 6:4, 7:3) and di-*o*-nitrobenzaldehyde **1** (250.27 mg, 0.5 mmol) were dissolved in THF (1 mL). After adding 1,6-diisocyanohexane (68.1 mg, 0.5 mmol), the tube was sealed under nitrogen. The initially heterogeneous mixture, due to the poor solubility of di-*o*-nitrobenzaldehyde **1**, became homogeneous in about 1 h, indicating the gradual conversion of monomers. The polymerization was conducted at 40 °C for 48 h. Afterward, the solution was immediately diluted with THF, and precipitated into diethyl ether. The obtained polymer was dried in vacuum and kept in a desiccator.

2.7. UV irradiated degradation of the polymers in solution

All the UV irradiation experiments were carried out under a Spectroline SB-100P/F high-intensity UV lamp (100 W, 365 nm). The solution of **PA-0** in $CDCl_3$ (10 mg/mL) was put on a platform at a distance of 10 cm under the lamp. The degradation was monitored by ^1H NMR at 0 h, 2 h, 4 h, 6 h, 8 h and 18 h intervals. After irradiation for 18 h, the supernatant was also examined by GPC.

2.8. UV irradiated degradation of the polymer film

The bulk degradation of polymer film upon UV irradiation was monitored by either UV–Vis or FTIR spectrometer. The polymer film was obtained by drop casting the solution of **PA-0.4** in THF onto the quartz plate or KBr disk. After removal of solvent via evaporation, the sample was placed on a platform at a distance of 10 cm under the UV lamp. UV–Vis spectra were recorded on a Shimadzu 2101 UV–Vis spectrometer. FTIR spectra were recorded by a Bruker Vector22 FTIR spectrometer. The degradation of the bulk film was monitored at 0 h, 2 h, 4 h, 6 h, 8 h, 10 h and 24 h intervals.

2.9. Adhesion test

Adhesion properties were determined by lap shear strength test. Glass plates ($76.2 \times 25.4 \times 0.8$ mm^3) were chosen as substrates to ensure the transmission of light. Prior to mount the adhesives, the glass plates were washed with acetone and sonicated for three times, and air-dried overnight. Polymer solution (50 μL) in THF (40 mg/mL) was uniformly applied to the adherend. The adherend contact area was 25.4×25.4 mm^2. The specimen was clamped for 12 h and then dried in vacuo. The adhesion strength tests were performed using an Instron 5567 testing machine with a 1 kN load cell. Load was recorded as a function of displacement with a crosshead speed of 2 mm/min. The maximum load was then divided by the contact area to calculate the adhesion strength. For each sample, lap shear strength was measured at least seven times, averaged and reported with error bars showing standard deviation. For the typical UV dismantlable behavior, the specimen adhered by **PA-0.4** was placed on a platform at a distance of 10 cm under the UV lamp. After irradiation for 24 h, lap shear strength was tested. Data were repeated for five times.

3. Results and discussion

3.1. Polymer synthesis and characterization

In our previous reports, we found that the Passerini MCP of a diisocyanide, a dicarboxylic acid and an *o*-nitrobenzaldehyde could efficiently generate UV degradable polymers, demonstrating that *o*-nitrobenzaldehyde is a highly reactive aldehyde towards this polymerization [59,60]. To examine whether the catechol group is compatible with this polymerization process, we first carried out the model Passerini reaction of 3-(3,4-dihydroxyphenyl) propionic acid, 5-ethoxy-2-nitrobenzaldehyde and *tert*-butyl isocyanide. Thus, these three compounds were dissolved in THF, and the mixture was heated to 40 °C with vigorous stirring. The reaction mixture was homogeneous at the beginning, but it gradually became heterogeneous. After 48 h, the mixture was poured into diethyl ether, and the precipitate was collected, washed with diethyl ether to get compound **2** in 80% yield (Fig. 1). Characterization by NMR spectrum confirmed the expected product, thus demonstrating that the catechol group is compatible with the Passerini reaction.

Encouraged by this model reaction, we synthesized the di-*o*-nitrobenzaldehyde derivative monomer **1**. 1, 12-Dibromo-dodecane was used as a linker of the two *o*-nitrobenzaldehydes, because this long alkyl chain can increase the polymer chain flexibility and thus reduce the glass transition temperature (T_g) of the resulting polymer. Simple treatment of 5-hydroxy-2-nitrobenzaldehyde with 1, 12-dibromododecane in DMF in the presence of potassium carbonate afforded **1** in 52% yield (Fig. S2). Then, the Passerini MCP was conducted using monomer **1**, 1,6-diisocyanohexane, and undecanoic acid (molar ratio 1: 1: 2) in $CHCl_3$ or THF. In both solvents, polymers were obtained as expected as confirmed by ^1H NMR spectrum (Fig. 2), the polymers from $CHCl_3$ showed slightly higher molecular weight (Table 1).

We next prepared seven polymers with variable catechol contents to examine their adhesion properties. The interaction of catechol moieties with many surfaces was well documented in the literature [21–23]. Using 3-(3,4-dihydroxyphenyl) propionic acid as a functional carboxylic acid could endow the obtained polymers with pendant catechol groups, which would enhance adhesion. Besides, we chose undecanoic acid as a comonomer not only to change the content of pendant catechol groups, but also to further adjust the T_g of the polymers. The polymerization of **1**, 1,6-diisocyanohexane, 3-(3,4-dihydroxyphenyl) propionic acid, and undecanoic acid with different carboxylic acids feed ratios was conducted in THF at 40 °C for 3 days. Though $CHCl_3$ seemed more appropriate according to the aforementioned results with a slight higher molecular weight of the final polymer, we had to choose THF as the reaction medium, owing to the poor solubility of 3-(3,4-dihydroxyphenyl) propionic acid in $CHCl_3$. The obtained polymers were characterized by ^1H NMR (Fig. 3, Fig. S3). From the ^1H NMR

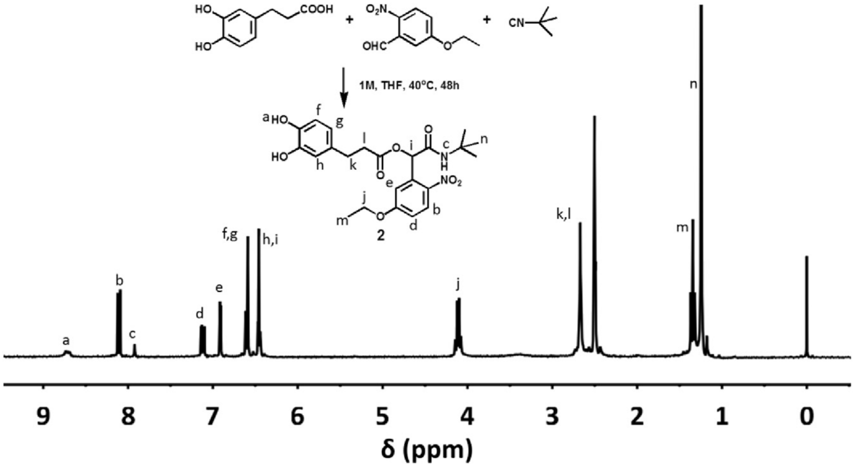

Fig. 1. ^{1}H NMR spectrum of model compound **2**.

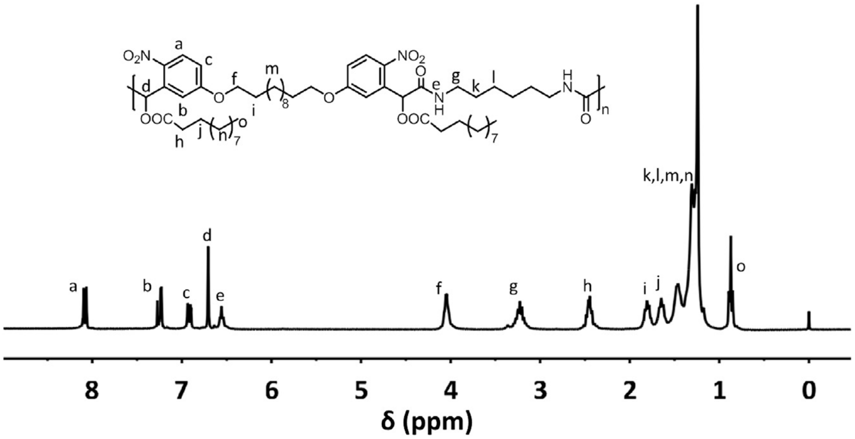

Fig. 2. ^{1}H NMR spectrum of **PA-0** in $CDCl_3$.

spectra, we could observe the gradual increase of proton signals corresponding to the catechol groups (c, e, g, k, l) with the increase of the feed ratio of 3-(3,4-dihydroxyphenyl) propionic acid. In addition, the calculated catechol content in the polymer *via* the comparison between the integration of methylene protons (k, l) and methyl protons (t) was in good accordance with the feed ratio. However, with more 3-(3,4-dihydroxyphenyl) propionic acid incorporated, such as polymers **PA-0.6** and **PA-0.7**, the solubility of the obtained polymer decreased, and we had to use DMSO-d_6 instead of $CDCl_3$ to confirm the polymer structure by NMR measurement (Fig. S3). The GPC data of these two polymers could not be evaluated due to the poor solubility. Molecular weights of other polymers are summarized in Table 1.

Thermal properties of all the polymers were investigated by TGA and DSC (Table 1, Fig. 4 and Fig. S4). From the TGA traces, we could see a two-stage decomposition, which was ascribed to the pyrolysis

Table 1
Characterizations of polymers obtained by Passerini MCP.

Entry	Catechol (%)		M_n (kDa)[e]	PDI[e]	Yield (%)[f]	T_d (°C)	T_g (°C)	Lap shear strength (Mpa)
	Feed	Polymer[d]						
PA-0[a]	0	0	11.1	1.59	70	293	16.9	–
PA-0[b]	0	0	7.7	1.64	52	290	14.0	0.22 ± 0.05
PA-0.1	10	9.1	6.5	1.71	71	281	28.4	0.30 ± 0.11
PA-0.2	20	22.8	14.2	2.12	79	276	37.8	0.34 ± 0.12
PA-0.3	30	34.9	10.4	2.59	92	271	45.6	0.49 ± 0.04
PA-0.4	40	44.2	8.6	1.73	86	267	50.0	0.46 ± 0.05
PA-0.5	50	48.3	9.2	2.76	93	260	55.1	0.53 ± 0.07
PA-0.6[c]	60	64.5	–	–	91	259	65.1	–
PA-0.7[c]	70	69.4	–	–	94	249	70.4	–

[a] Polymerization was carried out in $CHCl_3$.
[b] Polymerization was carried out in THF.
[c] The M_n, PDI and lap shear strength were not determined due to the poor solubility of polymers.
[d] The catechol contents in polymer were calculated by the integration of relevant ^{1}H NMR spectra.
[e] Measured by GPC in THF.
[f] Determined by precipitation into diethyl ether and vacuum dryness.

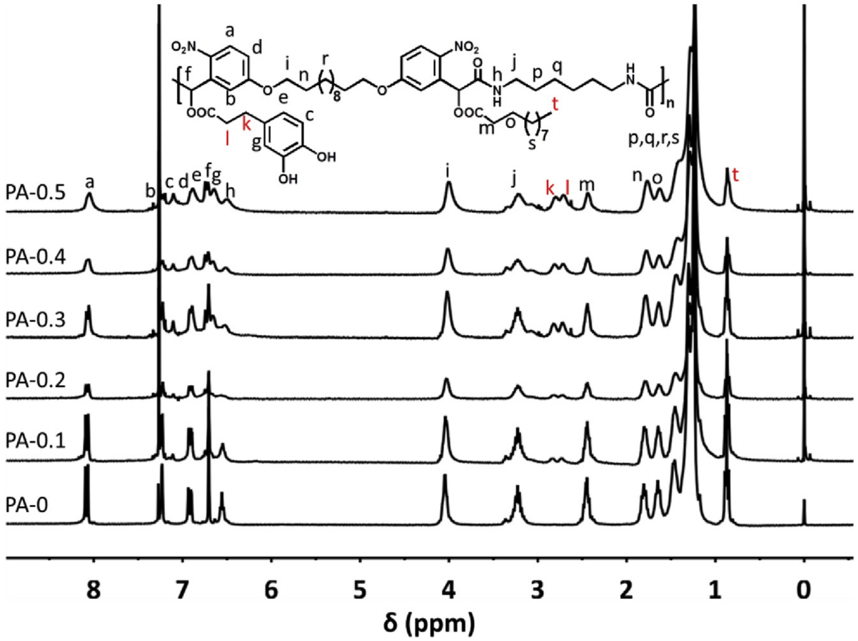

Fig. 3. ^{1}H NMR spectra of polymers with varied catechol contents.

of the ester bond and amide linkage respectively. The calculated value of the first-stage weight loss was 36%, which was in good accordance with the theoretical value (33%), when the ester bond was decomposed (Fig. 4(a)). Increase of catechol content could lower the decomposition temperature and increase the T_g of the polymers.

3.2. UV irradiated degradation of copolymers

One distinctive feature of the obtained polymers is the photodegradability due to the incorporated *o*-nitrobenzyl ester groups. Studies show that this structure can be facilely cleaved upon UV irradiation [47,48]. Therefore, all the prepared polymers are expected to decompose via UV irradiation, providing the unique debonding characteristic of the adhesives. Herein, the degradation behavior of these polymers was characterized by ^{1}H NMR, GPC, UV–Vis and FTIR analysis.

Initially, the UV degradation behavior of **PA-0** in $CDCl_3$ (10 mg/mL) was monitored by ^{1}H NMR measurements with different UV irradiation time (365 nm, 100 w) (Fig. 5a). A regular change of the corresponding proton signals could be observed.

The peak of methine proton (a, 6.70 ppm) ascribed to the *o*-nitrobenzyl ester group gradually disappeared within 18 h. Meanwhile the methylene protons (b, 2.44 ppm) adjacent to the pendant ester bond gradually shifted to the higher field (c, 2.35 ppm), indicating the photo-cleaved release of undecanoic acid. It should be noted that after 2 h irradiation, the initial homogeneous solution became heterogeneous, with a clear observation of brown solid. The amount of this solid increased with irradiation time. Owing to the poor solubility, we could not identify the chemical structure of this solid. This phenomenon also revealed the intrinsic complexity of this photochemical reaction. From the NMR spectra, we are quite sure that the solids are the degradation products containing mainly the aromatic fragments. Since the signals of methylene protons (d, 3.22 ppm) adjacent to the amide bonds were still present in the ^{1}H NMR spectra, though with a slight decrease of integration, we anticipated that the polymer was degraded into three parts. As was well known, *o*-nitrobenzyl ester could be cleaved by UV irradiation and afford the corresponding carboxylic acid and *o*-nitrosobenzaldehyde [47,48]. In this work, we observed the formation of undecanoic acid. The residue backbone should contain α-keto amide linkages (Scheme 2). According to the literature [70], this

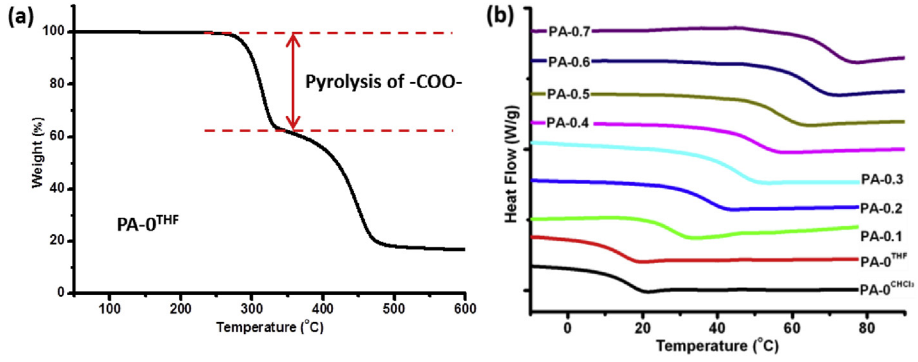

Fig. 4. (a) One typical TGA curve of **PA-0** polymerized in THF and (b) stacked DSC curves of polymers with varied catechol contents.

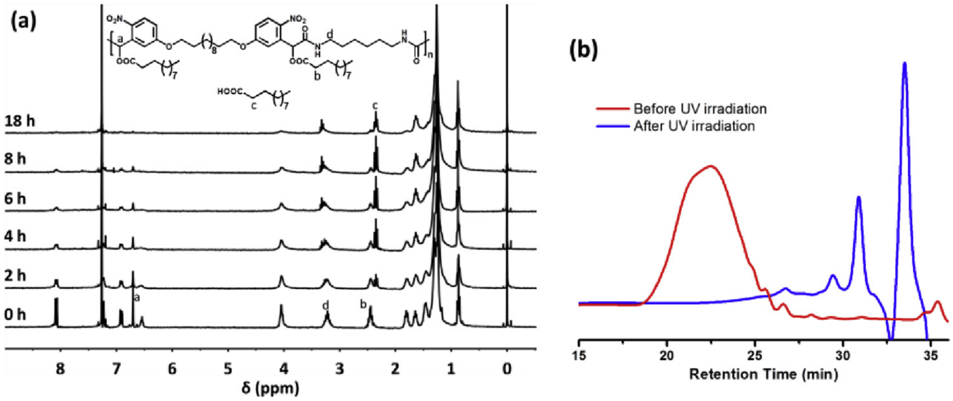

Fig. 5. (a) ^{1}H NMR spectra of **PA-0** upon UV irradiation. (b) GPC traces of **PA-0** before and after UV irradiation.

structure could further undergo photochemical reaction to ensure the degradation of the polymer backbone. GPC measurements revealed the absence of high molecular weight products in the supernatant of the **PA-0** solution after UV irradiation (Fig. 5(b)). Collectively, these data demonstrated that at least most part of the polymer main chain had been photo-cleaved.

Considering the practical application of adhesives, we also studied the UV degradation behavior of these polymers in bulk. At first, we measured the maximum absorption of catechol and *o*-nitrobenzyl ester groups by comparing the UV–Vis absorption spectra of 3-(3,4-dihydroxyphenyl) propionic acid, **PA-0** and **PA-0.4** in THF (0.04 mg/mL) (Fig. 6(a)). Catechol group had a typical absorption peak at around 280 nm. **PA-0** had a maximum absorption at around 310 nm, which was ascribed to the *o*-nitrobenzyl ester group. The two distinguishing peaks of **PA-0.4** are consistent with the presence of two functionalities. Since catechol did not show any absorbance at around 365 nm, which was the operating wavelength of the UV lamp, it would not inhibit the photoreaction of *o*-nitrobenzyl ester group. When the thin film of **PA-0.4** was irradiated with a UV lamp for different time, a gradual decrease of the absorption peak of *o*-nitrobenzyl ester at 310 nm was observed, while new absorption bands at 400–500 nm gradually increased with the formation of *o*-nitrosobenzaldehyde (Fig. 6(b)) [47,48].

Besides, FTIR analysis was also employed to monitor the UV degradation of **PA-0.4** in bulk (Fig. 7). After UV irradiation for 24 h, we could notice the gradual decrease of peaks at 1747 cm^{-1} and 1348 cm^{-1}, which were ascribed to the carbonyl stretching of the ester bond and the N–O stretching of nitro group, respectively. Though the newly formed undecanoic acid could not be clearly observed due to the overlay of the O–H stretching of carboxylic acid and catechol above 3000 cm^{-1}, the regular change of FTIR spectra revealed the photoreaction of polymer film upon UV irradiation. These results confirm that these polymers can also be photo-cleaved in the solid state.

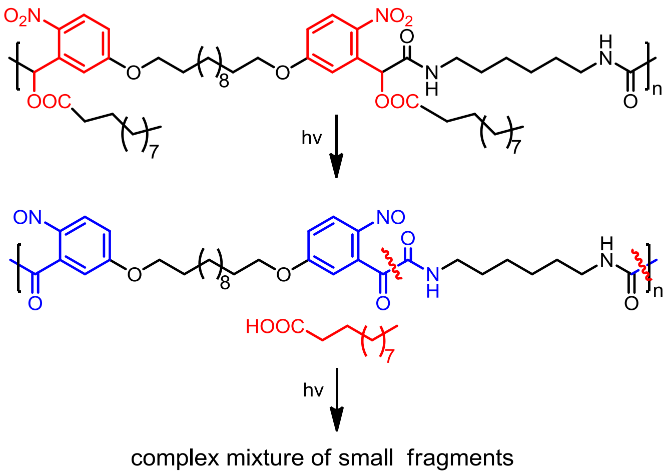

Scheme 2. Proposed mechanism of photocleavage of **PA-0** [47,48,70].

3.3. Application to dismantlable adhesives

The adhesion performance of the polymers containing different catechol groups was investigated by lap shear strength test. Glass plates were chosen as adherends to ensure that the majority of light can pass through. In this way, the subsequent UV dismantlable process could be achieved by just putting a UV lamp upon the glass plates. The adhesion test was conducted by uniformly placing the polymer solution in THF between two substrates. After removal of THF by evaporation in vacuo, the specimen was mounted on an Instron testing machine and pulled to failure. The typical result for **PA-0.5** is shown in Fig. 8(a). With the extension of displacement, the force gradually reached its maximum value. The sudden drop of force indicated the failure of the specimen, and the maximum load was divided by the overlapping contact area to calculate the adhesion strength.

To examine the influence of catechol contents on the adhesive performance, we measured the bulk adhesion strength for each of the polymers, except for **PA-0.6** and **PA-0.7**, due to their poor solubility in THF. Fig. 8(b) revealed that polymers with more catechol groups displayed relatively larger adhesion strength, with that of **PA-0** being 0.22 ± 0.05 MPa, while that of **PA-0.5** being 0.53 ± 0.07 MPa, 240% of **PA-0**. The adhesion strengths of **PA-0.3**, **PA-0.4**, and **PA-0.5** are quite similar, thus demonstrating that a maximum plateau may be reached in **PA-0.3**. This DOPA derivative has been incorporated into many synthetic adhesives [8–11,14,15], and the amount of catechol contents in the polymer can influence the adhesion performance dramatically. Theoretically, more catechol groups can provide more interaction with the substrate, thus enhance the adhesion force. Besides, an increase in catechol content also increases T_g. The modulus of adhesive layer, i. e. lap shear strength could also be improved as well. However, in our case, the observed adhesion strength did not increase constantly with the increase of catechol groups. As documented in the literature [1], the measured energy during separation of the adherends is a complex function of the adhesion energy and the dissipative properties. When a force is applied to the system, some energy is dissipated by the chain movement. In the current study, too much catechol groups could lead to the extensive increase of T_g, which in turn

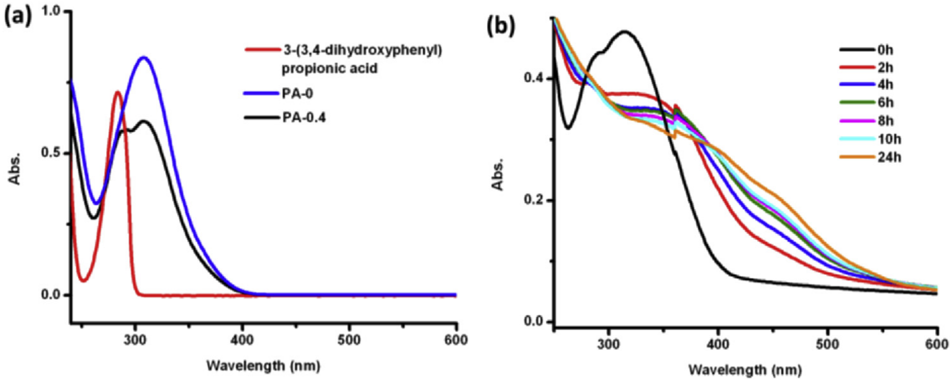

Fig. 6. (a) UV–Vis absorption spectra of 3-(3,4-dihydroxyphenyl) propionic acid, **PA-0** and **PA-0.4** in THF (0.04 mg/mL). (b) UV–Vis absorption spectra of bulk **PA-0.4** recorded as a function of UV exposure time (365 nm, 100 w).

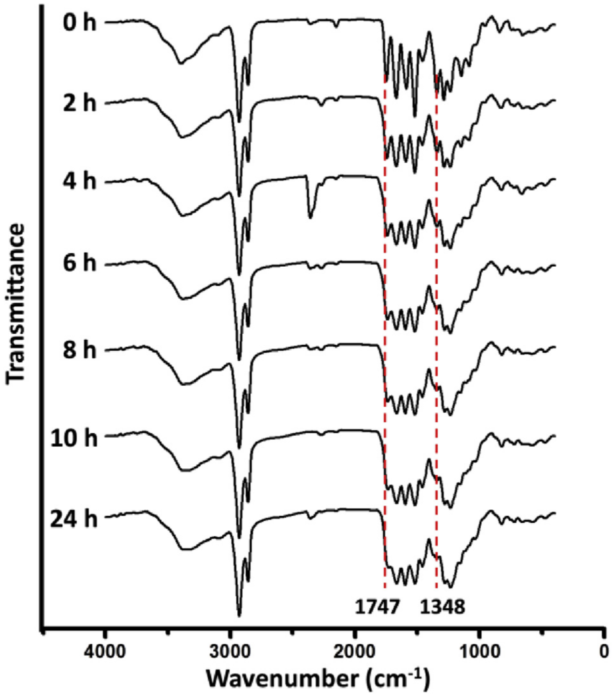

Fig. 7. FTIR spectra of **PA-0.4** upon UV irradiation.

prevents the motion of molecular chains. The decrease of dissipation energy leads to the decreased adhesion strength. Therefore, the results shown in Fig. 8(b) were the compromised results of catechol interaction and chain movement.

Finally, **PA-0.4** was selected as a representative example to test the UV dismantlable properties of the adhesives. The reason we chose **PA-0.4** was because the adhesion strength of **PA-0.4** was in the middle of the maximum plateau, indicating a possible appropriate balance between catechol interaction and chain dissipation during use. From the aforementioned ^{1}H NMR results, the UV degradation of **PA-0** took about 18 h to complete. Thus, the specimen adhered by **PA-0.4** was irradiated for 24 h to ensure a full degradation of the polymer. Upon UV irradiation, the initially colorless adhesive became gradually brown (data not shown), which was contributed to the conversion of nitro groups into nitroso counterparts. The lap shear strength test of the UV debonded specimen was carried out under the same condition as mentioned above. From Fig. 8(c), an obvious change of adhesion properties of **PA-0.4** could be noticed. The adhesion strength after UV irradiation (0.25 ± 0.03 MPa) was 54% of the original value (0.46 ± 0.05 MPa), revealing the UV dismantlability of the polymers.

4. Conclusions

Polymers consisting of varied catechol moieties and *o*-nitrobenzyl ester groups were successfully synthesized by the Passerini MCP of a di-*o*-nitrobenzaldhyde derivative monomer, 1,6-diisocyanohexane, 3-(3,4-dihydroxyphenyl) propionic acid and undecanoic acid. Incorporation of dual functionalities endowed the polymers with adhesion and UV degradation properties. Adjusting the catechol contents in the polymers could tune the adhesion strengths to glass substrates. UV irradiation could cleave the polymer main chain and deteriorate the corresponding adhesion performance. It should be pointed out that the limitation of the application should be only for transparent substrates and the adhesive properties should be further improved by molecular design,

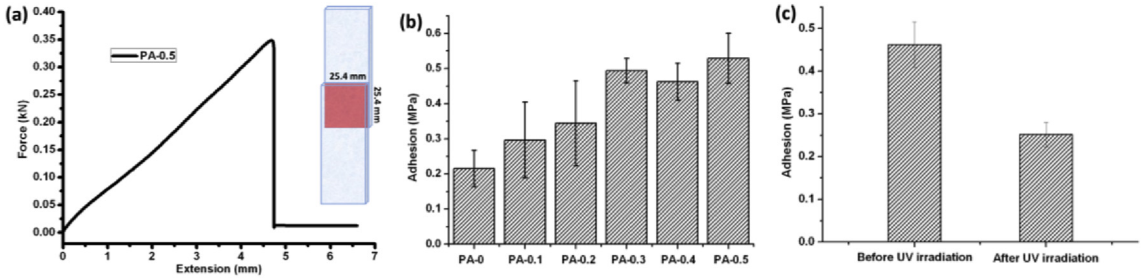

Fig. 8. (a) One typical force versus displacement curve reported by the Instron testing machine, (b) Lap shear strength of adhesives with varied catechol contents and (c) lap shear strength of **PA-0.4** before and after UV irradiation.

for example further lower the T_g of the polymers. Nevertheless, this is a simple approach to prepare UV dismantlable adhesives, and this approach may also extend to thermal dismantlable adhesives.

Acknowledgments

This work is financially supported by National Natural Science Foundation of China (No. 21090351 and 21225416) and National Basic Research Program of China (No. 2011CB201402).

Appendix A. Supplementary data

Supplementary data related to this article can be found at http://dx.doi.org/10.1016/j.polymer.2015.05.032.

References

[1] A. Baldan, Adhesively-bonded joints and repairs in metallic alloys, polymers and composite materials: adhesives, adhesion theories and surface pretreatment, J Mater Sci 39 (1) (2004) 1–49.
[2] B.P. Lee, P.B. Messersmith, J.N. Israelachvili, J.H. Waite, Mussel-inspired adhesives and coatings, in: D.R. Clarke, P. Fratzl (Eds.), Annual review of materials research, vol. 41, 2011, pp. 99–132.
[3] Q. Ye, F. Zhou, W. Liu, Bioinspired catecholic chemistry for surface modification, Chem Soc Rev 40 (7) (2011) 4244–4258.
[4] J. Sedo, J. Saiz-Poseu, F. Busque, D. Ruiz-Molina, Catechol-based biomimetic functional materials, Adv Mater 25 (5) (2013) 653–701.
[5] E. Faure, C. Falentin-Daudre, C. Jerome, J. Lyskawa, D. Fournier, P. Woisel, et al., Catechols as versatile platforms in polymer chemistry, Prog Polym Sci 38 (1) (2013) 236–270.
[6] M.E. Yu, T.J. Deming, Synthetic polypeptide mimics of marine adhesives, Macromolecules 31 (15) (1998) 4739–4745.
[7] H. Lee, B.P. Lee, P.B. Messersmith, A reversible wet/dry adhesive inspired by mussels and geckos, Nature 448 (7151) (2007) 338–341.
[8] C.E. Brubaker, P.B. Messersmith, Enzymatically degradable mussel-inspired adhesive hydrogel, Biomacromolecules 12 (12) (2011) 4326–4334.
[9] G. Westwood, T.N. Horton, J.J. Wilker, Simplified polymer mimics of cross-linking adhesive proteins, Macromolecules 40 (11) (2007) 3960–3964.
[10] C.R. Matos-Perez, J.D. White, J.J. Wilker, Polymer composition and substrate influences on the adhesive bonding of a biomimetic, cross-linking polymer, J Am Chem Soc 134 (22) (2012) 9498–9505.
[11] H. Chung, R.H. Grubbs, Rapidly cross-linkable DOPA containing terpolymer adhesives and PEG-based cross-linkers for biomedical applications, Macromolecules 45 (24) (2012) 9666–9673.
[12] C.L. Jenkins, H.J. Meredith, J.J. Wilker, Molecular weight effects upon the adhesive bonding of a mussel mimetic polymer, Acs Appl Mater Interf 5 (11) (2013) 5091–5096.
[13] J.H. Cho, K. Shanmuganathan, C.J. Ellison, Bioinspired catecholic copolymers for antifouling surface coatings, Acs Appl Mater Interf 5 (9) (2013) 3794–3802.
[14] J. Nishida, M. Kobayashi, A. Takahara, Light-triggered adhesion of water-soluble polymers with a caged catechol group, Acs Macro Lett 2 (2) (2013) 112–115.
[15] E.M. White, J.E. Seppala, P.M. Rushworth, B.W. Ritchie, S. Sharma, J. Locklin, Switching the adhesive state of catecholic hydrogels using phototitration, Macromolecules 46 (22) (2013) 8882–8887.
[16] K. Numata, P.J. Baker, Synthesis of adhesive peptides similar to those found in blue mussel (mytilus edulis) using papain and tyrosinase, Biomacromolecules 15 (8) (2014) 3206–3212.
[17] P. Wilke, N. Helfricht, A. Mark, G. Papastavrou, D. Faivre, H.G. Boerner, A direct biocombinatorial strategy toward next generation, mussel-glue inspired saltwater adhesives, J Am Chem Soc 136 (36) (2014) 12667–12674.
[18] S. Moulay, Dopa/catechol-tethered polymers: bioadhesives and biomimetic adhesive materials, Polym Rev 54 (3) (2014) 436–513.
[19] Q. Lin, D. Gourdon, C. Sun, N. Holten-Andersen, T.H. Anderson, J.H. Waite, et al., Adhesion mechanisms of the mussel foot proteins mfp-1 and mfp-3, Proc Natl Acad Sci 104 (10) (2007) 3782–3786.
[20] M.J. Harrington, A. Masic, N. Holten-Andersen, J.H. Waite, P. Fratzl, Iron-clad fibers: a metal-based biological strategy for hard flexible coatings, Science 328 (5975) (2010) 216–220.
[21] M.E. Yu, J.Y. Hwang, T.J. Deming, Role of L-3,4-dihydroxyphenylalanine in mussel adhesive proteins, J Am Chem Soc 121 (24) (1999) 5825–5826.
[22] H. Lee, N.F. Scherer, P.B. Messersmith, Single-molecule mechanics of mussel adhesion, Proc Natl Acad Sci 103 (35) (2006) 12999–13003.
[23] T.H. Anderson, J. Yu, A. Estrada, M.U. Hammer, J.H. Waite, J.N. Israelachvili, The contribution of DOPA to substrate-peptide adhesion and internal cohesion of mussel-inspired synthetic peptide films, Adv Funct Mater 20 (23) (2010) 4196–4205.
[24] L.J. Wang, H.Y. Li, C.P. Wong, Syntheses and characterizations of thermally reworkable epoxy resins II, J Polym Sci Polym Chem 38 (20) (2000) 3771–3782.
[25] J. Malik, S.J. Clarson, A thermally reworkable UV curable acrylic adhesive prototype, Int J Adhes Adhes 22 (4) (2002) 283–289.
[26] Y. Nishiyama, N. Uto, C. Sato, H. Sakurai, Dismantlement behavior and strength of dismantlable adhesive including thermally expansive particles, Int J Adhes Adhes 23 (5) (2003) 377–382.
[27] J.H. Aubert, Thermally removable epoxy adhesives incorporating thermally reversible Diels-Alder adducts, J Adhes 79 (6) (2003) 609–616.
[28] H. Ishikawa, K. Seto, S. Shimotuma, N. Kishi, C. Sato, Bond strength and debonding behavior of elastomer and emulsion-type dismantlable adhesives used for building materials, Int J Adhes Adhes 25 (3) (2005) 193–199.
[29] T. Xie, X. Xiao, Self-peeling reversible dry adhesive system, Chem Mater 20 (9) (2008) 2866–2868.
[30] R. Wang, T. Xie, Shape memory- and hydrogen bonding-based strong reversible adhesive system, Langmuir 26 (5) (2010) 2999–3002.
[31] R. Wang, X. Xiao, T. Xie, Viscoelastic behavior and force nature of thermo-reversible epoxy dry adhesives, Macromol Rapid Commun 31 (3) (2010) 295–299.
[32] X. Luo, K.E. Lauber, P.T. Mather, A thermally responsive, rigid, and reversible adhesive, Polymer 51 (5) (2010) 1169–1175.
[33] E. Sato, H. Tamura, A. Matsumoto, Cohesive force change induced by polyperoxide degradation for application to dismantable adhesion, Acs Appl Mater Interf 2 (9) (2010) 2594–2601.
[34] E. Sato, T. Hagihara, A. Matsumoto, Facile synthesis of main-chain degradable block copolymers for performance enhanced dismantlable adhesion, Acs Appl Mater Interf 4 (4) (2012) 2057–2064.
[35] K. Ebe, H. Seno, K.U.V. Horigome, curable pressure-sensitive adhesives for fabricating semiconductors. I. Development of easily peelable dicing tapes, J Appl Polym Sci 90 (2) (2003) 436–441.
[36] S.R. Trenor, T.E. Long, B.J. Love, Development of a light-deactivatable PSA via photodimerization, J Adhes 81 (2) (2005) 213–229.
[37] T. Inui, E. Sato, A. Matsumoto, Pressure-sensitive adhesion system using acrylate block copolymers in response to photoirradiation and postbaking as the dual external stimuli for on-demand dismantling, Acs Appl Mater Interf 4 (4) (2012) 2124–2132.
[38] M. Kobayashi, M. Terada, A. Takahara, Reversible adhesive-free nanoscale adhesion utilizing oppositely charged polyelectrolyte brushes, Soft Matter 7 (12) (2011) 5717–5722.
[39] B.J. Adzima, Y. Tao, C.J. Kloxin, C.A. DeForest, K.S. Anseth, C.N. Bowman, Spatial and temporal control of the alkyne-azide cycloaddition by photoinitiated Cu(II) reduction, Nat Chem 3 (3) (2011) 256–259.
[40] C.A. DeForest, K.S. Anseth, Cytocompatible click-based hydrogels with dynamically tunable properties through orthogonal photoconjugation and photocleavage reactions, Nat Chem 3 (12) (2011) 925–931.
[41] A.M. Kloxin, A.M. Kasko, C.N. Salinas, K.S. Anseth, Photodegradable hydrogels for dynamic tuning of physical and chemical properties, Science 324 (5923) (2009) 59–63.
[42] D.R. Griffin, A.M. Kasko, Photodegradable macromers and hydrogels for live cell encapsulation and release, J Am Chem Soc 134 (31) (2012) 13103–13107.
[43] D.R. Griffin, A.M. Kasko, Photoselective delivery of model therapeutics from hydrogels, Acs Macro Lett 1 (11) (2012) 1330–1334.
[44] H. Zhao, E.S. Sterner, E.B. Coughlin, P. Theato, o-Nitrobenzyl alcohol derivatives: opportunities in polymer and materials science, Macromolecules 45 (4) (2012) 1723–1736.
[45] J.-F. Gohy, Y. Zhao, Photo-responsive block copolymer micelles: design and behavior, Chem Soc Rev 42 (17) (2013) 7117–7129.
[46] C.P. Holmes, D.G. Jones, Reagents for combinatorial organic-synthesis – development of a new o-nitrobenzyl photolabile linker for solid-phase synthesis, J Org Chem 60 (8) (1995) 2318–2319.
[47] A.P. Pelliccioli, J. Wirz, Photoremovable protecting groups: reaction mechanisms and applications, Photochem Photobiol Sci 1 (7) (2002) 441–458.
[48] Y.V. Il'ichev, M.A. Schworer, J. Wirz, Photochemical reaction mechanisms of 2-nitrobenzyl compounds: methyl ethers and caged ATP, J Am Chem Soc 126 (14) (2004) 4581–4595.
[49] A. Domling, I. Ugi, Multicomponent reactions with isocyanides, Angew Chem Int Ed 39 (18) (2000) 3169–3210.
[50] A. Domling, Recent developments in isocyanide based multicomponent reactions in applied chemistry, Chem Rev 106 (1) (2006) 17–89.
[51] A. Domling, W. Wang, K. Wang, Chemistry and biology of multicomponent reactions, Chem Rev 112 (6) (2012) 3083–3135.
[52] M. Passerini, I. Isonitriles, Compound of p-isonitrileazobenzene with acetone and acetic acid, Gazz Chim Ital 51 (1921) 126–129.
[53] J.G. Rudick, Innovative macromolecular syntheses via isocyanide multicomponent reactions, J Polym Sci Polym Chem 51 (19) (2013) 3985–3991.
[54] R. Kakuchi, Multicomponent reactions in polymer synthesis, Angew Chem Int Ed 53 (1) (2014) 46–48.
[55] X.-X. Deng, L. Li, Z.-L. Li, A. Lv, F.-S. Du, Z.-C. Li, Sequence regulated poly(ester-amide)s based on passerini reaction, Acs Macro Lett 1 (11) (2012) 1300–1303.
[56] Y.-Z. Wang, X.-X. Deng, L. Li, Z.-L. Li, F.-S. Du, Z.-C. Li, One-pot synthesis of polyamides with various functional side groups via Passerini reaction, Polym Chem 4 (3) (2013) 444–448.
[57] A. Lv, X.-X. Deng, L. Li, Z.-L. Li, Y.-Z. Wang, F.-S. Du, et al., Facile synthesis of multi-block copolymers containing poly(ester-amide) segments with an ordered side group sequence, Polym Chem 4 (13) (2013) 3659–3662.
[58] L.-J. Zhang, X.-X. Deng, F.-S. Du, Z.-C. Li, Chemical synthesis of functional poly(4-hydroxybutyrate) with controlled degradation via intramolecular cyclization, Macromolecules 46 (24) (2013) 9554–9562.

[59] L. Li, A. Lv, X.-X. Deng, F.-S. Du, Z.-C. Li, Facile synthesis of photo-cleavable polymers via Passerini reaction, Chem Commun 49 (76) (2013) 8549–8551.
[60] L. Li, X.-X. Deng, Z.-L. Li, F.-S. Du, Z.-C. Li, Multifunctional photodegradable polymers for reactive micropatterns, Macromolecules 47 (14) (2014) 4660–4667.
[61] X.-X. Deng, F.-S. Du, Z.-C. Li, Combination of orthogonal ABB and ABC multicomponent reactions toward efficient divergent synthesis of dendrimers with structural diversity, Acs Macro Lett 3 (7) (2014) 667–670.
[62] X.-X. Deng, Y. Cui, F.-S. Du, Z.-C. Li, Functional highly branched polymers from multicomponent polymerization (MCP) based on the ABC type Passerini reaction, Polym Chem 5 (10) (2014) 3316–3320.
[63] O. Kreye, T. Toth, M.A.R. Meier, Introducing multicomponent reactions to polymer science: passerini reactions of renewable monomers, J Am Chem Soc 133 (6) (2011) 1790–1792.
[64] A. Sehlinger, O. Kreye, M.A.R. Meier, Tunable polymers obtained from Passerini multicomponent reaction derived acrylate monomers, Macromolecules 46 (15) (2013) 6031–6037.
[65] A. Sehlinger, L.M. de Espinosa, M.A.R. Meier, Synthesis of diverse asymmetric alpha,omega-dienes via the Passerini three-component reaction for head-to-tail ADMET polymerization, Macromol Chem Phys 214 (24) (2013) 2821–2828.
[66] A. Sehlinger, R. Schneider, M.A.R. Meier, Passerini addition polymerization of an AB-type monomer - a convenient route to versatile polyesters, Eur Polym J 50 (2014) 150–157.
[67] S.C. Solleder, M.A.R. Meier, Sequence control in polymer chemistry through the Passerini three-component reaction, Angew Chem Int Ed 53 (3) (2014) 711–714.
[68] O. Kreye, D. Kugele, L. Faust, M.A.R. Meier, Divergent dendrimer synthesis via the Passerini three-component reaction and olefin cross-metathesis, Macromol Rapid Commun 35 (3) (2014) 317–322.
[69] J.-A. Jee, L.A. Spagnuolo, J.G. Rudick, Convergent synthesis of dendrimers via the Passerini three-component reaction, Org Lett 14 (13) (2012) 3292–3295.
[70] U. Zehavi, Photochemical reactions of phenylglyoxalyl amides, J Org Chem 42 (17) (1977) 2821–2825.